JOURNAL OF PROPULSION AND POWER
Vol. 12, No. 4, July–August 1996

Burn Time Measurements of Single Aluminum Particles in Steam and CO_2 Mixtures

S. E. Olsen* and M. W. Beckstead†
Brigham Young University, Provo, Utah 84602

In this study, single aluminum particles (40–80 μm) were burned in H_2O/CO_2 mixtures. Burn times were measured electronically using a photo multiplier tube. In addition, the effect of oxidizer composition was determined. Burn times were also measured for single particles, quenched at various stages of combustion. Scanning electron microscope micrographs of quenched specimens were obtained. The results were used in determining particle burn times. A study of quenched particles revealed the formation of large hollow aluminum oxide spheres nearly the size of the original aluminum particle. These spheres have been reported by other investigators at both atmospheric and high-pressure conditions. It was found that burn time measurements are very sensitive to the method of analysis used. Using the results of an aluminum combustion model (Brooks, K. P., and Beckstead, M. W., "Dynamics of Aluminum Combustion," *Journal of Propulsion and Power*, Vol. 11, No. 4, pp. 769, 770), effective oxygen concentrations were calculated for this work and other data. A relationship exists between the effective oxygen concentration and burn times reported for a given diameter. The particle burn times measured in this work compare well with other data if the effective oxygen concentration is properly accounted for.

Introduction

THE performance of most solid rocket propellants can be improved by the addition of aluminum powder. Aluminum reacts with certain products of propellant combustion, notably water and carbon dioxide, to give a substantial increase in the gas temperature. Motor acoustic stability is also influenced by the addition of aluminum powder. The addition of powdered metals has been found to be highly effective in suppressing acoustic instability in many rocket motors. However, in some cases, for reasons not well understood, aluminum addition appears to promote acoustic instability.[2] Further investigation into aluminum particle combustion is needed to assist in the formulation of a model.

The burn times of laser-ignited aluminum particles have been measured by Wilson and Williams.[3] Prentice[4] has also published data for flash and laser-ignited particles. Data in these studies were generally collected using single particles 50 μm in diameter[3] and 250–400 μm in diameter,[4] in ambient temperature gases of less than 30% oxygen diluted with Ar, N_2, and CO_2.

Several investigators have performed experiments involving burner-ignited aluminum particles. Drew et al.[5] investigated the ignition and burning geometry of aluminum particles in H_2/O_2 flames. Fassel and Papp[6] have reported burn times for the average diameter of several particle size distributions ranging from 15 to 32 μm. Davis[7] measured burn times for a distribution of particle sizes (53–66 μm) ignited in a $CO/O_2/N_2$ flame. Friedman and Macek[8–10] gave burn times for average particle diameters of 30–50 μm in propane/O_2/N_2 and $CO/O_2/N_2$ flames. More recently, Turns and Wong[11,12] have completed a study involving the combustion of aluminum slurry agglomerates, ranging from 300 to 800 μm in diameter, in the hot products region of a flat flame using cinematography.

Particle burn rates at high pressures (10–200 atm) were measured in propellant bomb experiments.[7,10,13,14] These experiments give burn time measurements for distributions of aluminum particles (20–100 μm nominally) ignited in propellant samples. Samples generally contained low concentrations of aluminum to eliminate agglomeration. Price et al.[15] have given an extensive report on the behavior of aluminum in solid propellant combustion. Tokui and Iwama[16] conducted x-ray analysis studies on aluminum particles quenched while burning at pressures up to 30 atm. Aluminum wire, wrapped around the tip of a quartz fiber, formed 3–4-mm aluminum spheres when ignited by joule heating or a small propellant flame. The burning particles were allowed to fall through an $Ar/N_2/O_2$ environment before quenching.

Burn time measurements for a nominal 20-μm size distribution of aluminum particles ignited by shock waves have been reported recently by Roberts et al.[17] They performed experiments by igniting 5000 to 10,000 particles simultaneously in oxygen at pressures up to 34 atm.

It is difficult to make a direct comparison of data from different investigators because of the widely different test conditions and test methods employed. However, various data have been normalized using a D^2 law and plotted in Fig. 1 to show the scatter existing in available data. The data scatter is not improved by changing the exponent of the particle diameter from 2 to 1.5 or 1.8. Furthermore, this plot does not allow an accounting for the variation in oxidizer nor inert gas concentrations between the various experiments.

Experimental Method

The purpose of this experiment was to measure combustion rates of single aluminum particles in an oxidizing environment similar to that of propellant.

Particle Collection

The determination of initial particle size is crucial to the experimental success, but is difficult to do accurately. The particles studied, typically involve relatively wide size distributions of very small, often nonspherical aluminum particles. To decrease the uncertainty involved in measuring the combustion times of aluminum particles, particles used in this experiment were individually sized and separated under a microscope. A collection probe was designed to collect small spherical par-

Presented as Paper 95-2715 at the AIAA/ASME/SAE/ASEE 31st Joint Propulsion Conference and Exhibit, San Diego, CA, July 10–12, 1995; received July 20, 1995; revision received Jan. 13, 1996; accepted for publication Feb. 2, 1996.

*Graduate Assistant, Department of Mechanical Engineering.
†Professor, Department of Chemical Engineering. Associate Fellow AIAA.

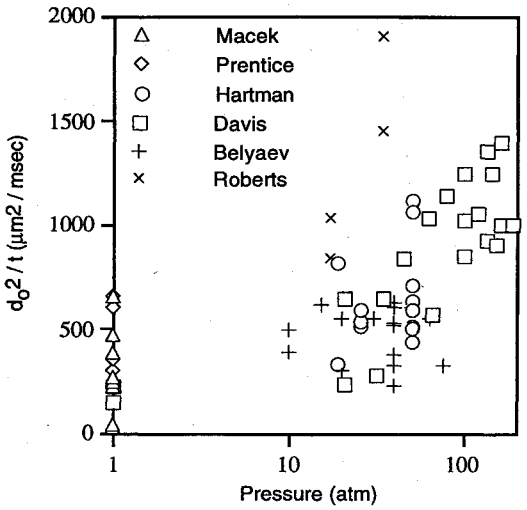

Fig. 1 Comparison of experimental data for burn rate of aluminum particles.

ticles individually. The probe consisted of a thin-walled glass capillary fiber fixed to the end of a pipette.

A rubber bulb attached to the pipette allowed single particles to be sucked up and held on the end of the fiber. Particles were released by squeezing the bulb to blow the particle off the end of the fiber. Particles were also attracted and held by electrostatic forces on the end of a glass fiber or by adhesion to oil from fingers rubbed on the fiber. The latter methods, however, did not allow as much control in manipulating the particle as the suction method.

Particles used were obtained from spherical atomized aluminum powder. Particles were measured using a tool-makers microscope with accuracy to 1 μm. Almost without exception the limiting factor in the accuracy attainable was the sphericity of the particles. For instance, 70-μm particles could be found whose roundness varied less than 3 μm from the nominal diameter. Smaller particles (40–50 μm) tended to be less spherical than the larger sizes.

Burner Design

A small diffusion flame burner was used to ignite the aluminum particles (Fig. 2). Although a diffusion flame was admittedly not the best choice for producing uniform burning conditions, it was more stable during operation at elevated pressures than a premixed flame. This was of importance since the burner was intended for use at both atmospheric and elevated pressures. Since the majority of particle combustion occurred beyond the reaction zone, use of the diffusion flame burner, over a premixed flame, was justified. The burner was shielded from ambient gases to provide a controlled environment.

Particles were released, individually, into the downward flow of the flame through a particle feed hole. A solenoid release mechanism synchronized with data acquisition equipment provided a means of controlling a particle to release at precisely determined times. The burner was fired into a combustion chamber 3.2 cm in diameter and approximately 30 cm long. The combustion process was monitored through a viewing window that was 20 cm long. Originally, the combustion chamber was designed to operate over a range of pressures, but eventually all tests were performed at 1-atm pressure.

Ignition Flame and Environmental Control

Experimental evidence suggests that the oxidizing environment in which particle combustion takes place has a significant effect on the combustion process.[18] It is not always possible to obtain the desired oxidizing environment during particle combustion experiments. This is particularly true of burner exper-

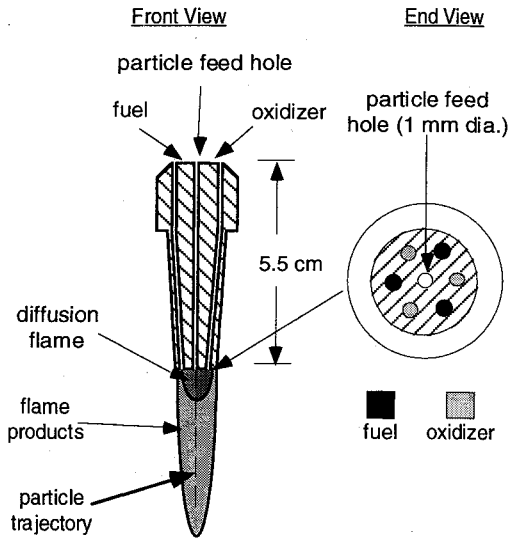

Fig. 2 Diffusion flame burner.

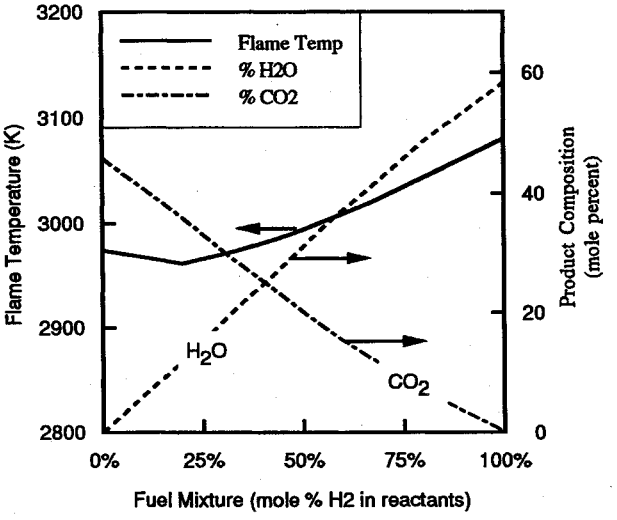

Fig. 3 Adiabatic flame temperature and product composition for various stoichiometric mixtures.

iments. In these experiments, the environmental composition in which particle combustion occurs is determined by the flame combustion products. Not all flames have sufficiently high temperatures to ignite aluminum particles. Flame temperatures must be at least as high as the melting point of aluminum oxide (approximately 2300 K) to ignite particles.

In this study it was desired to burn particles in an oxidizing environment characteristic of rocket motor conditions. Propellant combustion products consist mainly of H_2O, CO_2, and HCl. There is little molecular oxygen in the products. The following mole fractions are typically found in propellant combustion products: 0.35 H_2O, 0.17 CO, 0.09 CO_2, 0.18 HCl, 0.11 H_2, and 0.09 N_2. Of these products, H_2O and CO_2 are considered the most significant oxidizers available for combustion of aluminum. It is possible that both CO and OH could have an effect on the process, but they have not been considered in this, or previous, studies. It is readily apparent that oxygen is not an available oxidizing species in a solid propellant environment.

For this experiment an $H_2/CO/O_2$ flame was chosen to ignite the aluminum particles and provide a CO_2/H_2O oxidizing atmosphere. The adiabatic flame temperature for various fuel mixtures was calculated using the Edwards thermochemical equilibrium code and is plotted in Fig. 3. Calculations showed that use of an $H_2/CO/O_2$ flame provides an essentially constant

Table 1 Experimental test conditions and burn time data obtained for single aluminum particles

Particle diameter, μm	Feed composition, %			Fraction products[a]			Burn time, ms	Range, ± ms	Analysis method[b]
	CO	H_2	O_2	CO_2	H_2O	O_2			
40	0	64.5	35.5	0	0.89	0.11	3.3	0.65	1
40	0	64.5	35.5	0	0.89	0.11	4.2	0.52	2
40	0	64.5	35.5	0	0.89	0.11	3.4	0.42	3
50	0	64.5	35.5	0	0.89	0.11	3.9	0.62	1
50	0	64.5	35.5	0	0.89	0.11	4.5	0.56	2
50	0	64.5	35.5	0	0.89	0.11	3.7	0.42	3
60	0	64.5	35.5	0	0.89	0.11	4.8	0.61	1
60	0	64.5	35.5	0	0.89	0.11	5.2	0.66	2
60	0	64.5	35.5	0	0.89	0.11	4.3	0.46	3
70	0	64.5	35.5	0	0.89	0.11	6.3	0.80	1
70	0	64.5	35.5	0	0.89	0.11	6.3	0.80	2
70	0	64.5	35.5	0	0.89	0.11	5.3	0.56	3
80	0	64.5	35.5	0	0.89	0.11	8.8	1.00	1
80	0	64.5	35.5	0	0.89	0.11	8.6	1.10	2
80	0	64.5	35.5	0	0.89	0.11	7.0	0.65	3
70	9.7	54.8	35.5	0.08	0.79	0.13	7.6	0.89	1 and 2
70	9.7	54.8	35.5	0.08	0.79	0.13	6.3	0.84	3
70	19.4	45.2	35.5	0.18	0.66	0.16	8.5	1.00	1 and 2
70	19.4	45.2	35.5	0.18	0.66	0.16	6.8	0.89	3

[a]The oxidizer mole fraction calculated thermochemically for the gaseous flame products relative to the three oxidizing species (CO_2, H_2O, and O_2). Other products (CO, OH, H_2, and H, etc.) make up ~35% of the product gases.
[b]1, constant cutoff method; 2, percent peak height method; and 3, percent area method.

temperature flame (±50 K), for any stoichiometric mixture of O_2 and a fuel mixture of CO and H_2. The ability to provide an almost constant flame temperature for varying test conditions is very advantageous experimentally.

The product composition shown in Fig. 3 is for the two species, CO_2 and H_2O, that are considered as the primary oxidizing species for the subsequent aluminum combustion. To obtain the desired mixture of CO_2 and H_2O in the experiments, the input feed of CO, H_2, and O_2 was varied. An oxidizer mole fraction for CO_2, H_2O, or O_2 can be defined (e.g., X_{CO_2}), as

$$X_{CO_2} = \left(\frac{n_{CO_2}}{n_{H_2O} + n_{CO_2} + n_{O_2}} \right)$$

In an actual flame there are obviously other product species present because of dissociation and equilibrium conditions. Thus, for 100% H_2 as the fuel for the gaseous ignition flame, the product flame will consist of a mixture of H_2, O_2, H, OH, and H_2O, with 58% H_2O. For this example the value of X_{H_2O} is 1.0 as CO_2 and H_2O are the only product species considered in this plot. The feed compositions for the various tests are summarized in Table 1, as are the oxidizer mole fractions for the oxidizing species (calculated thermochemically for the gaseous flame products). The other gas products in the flame (i.e., CO, OH, H_2, and H, etc.) make up between 34–35% of the product gases, for the three conditions tested. In the actual tests, a rather sluggish ignition and combustion was observed for preliminary tests with atmospheres of primarily CO_2 and H_2O. Therefore, the actual testing was done with an excess of oxygen to ensure more complete combustion within the burner.

Data Acquisition

Radiative emission from burning aluminum particles was measured using a photo multiplier tube (PMT). A collection lens focused the particle image onto the PMT. A 383-nm bandpass interference filter was used to eliminate as much emission from the burner flame as possible. Initially, it was thought that specific aluminum emission lines could be measured, however, the graybody radiation overwhelmed the emission lines. Thus, the PMT was measuring the graybody radiation. The current signal generated by the PMT was converted to an amplified voltage signal by means of a transimpedance amplifier. A low-pass filter reduced high-frequency electrical noise. The data acquisition system aided in signal analysis and particle release mechanism control.

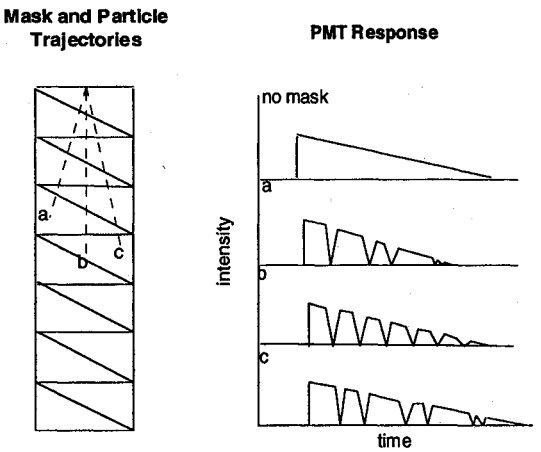

Fig. 4 Spatial locating mask concept.

Because the PMT alone measured only the variation of radiation intensity with time, it was helpful to devise a method whereby the particle could be tracked spatially in time. This was done to ensure that particles remained within the field of view (FOV) and that they followed regular trajectories. A light mask was constructed and placed on the viewing window between the PMT and the burning particle. Each time a particle passed a mask stripe the signal to the PMT was interrupted. Comparing the timing of the interruptions, the spatial location of the particle in time could be roughly determined. Figure 4 illustrates the principle. Several possible particle trajectories and the resulting signal responses are shown. A particle such as trace b with evenly spaced interruptions indicated that the particle was passing though the center of the combustion chamber. These tests showed that the particles did stay within the FOV, and that their trajectories were basically straight (not spiraling). Once satisfactory particle behavior was verified, the mask was removed for data acquisition.

Quenched Particle Studies

Past studies of quenched aluminum particles[4,6,18–22] have given an understanding of events that occur during particle combustion. With past data it is generally difficult to determine exactly when, during the combustion process, quenching occurred for a given specimen. In this study, single aluminum

particles were quenched by impacting onto glass slides during combustion while a simultaneous particle emission trace was recorded. This allowed the time between ignition and quenching to be measured.

Particle quenching was performed as follows. A single aluminum particle was sized and hand selected for sphericity by viewing under an optical microscope. The particle was released into the burner by a spring-loaded catapult system and ignited by the flame. A thin glass slide was inserted into the path of the particle trajectory resulting in the impact and quenching of the particle on the slide. Immediately after particle impact, the slide was withdrawn from the hot flame gases before excessive melting of the sample and slide occurred.

Many sampling attempts were required to collect a sufficient number of acceptable specimens representing the entire combustion process. Many attempts failed because specimens were distorted beyond recognition upon impact. Not all of the specimens surviving impact were oriented such that combustion details were revealed. Others were carried past the slide by the flow of gases, avoiding impact altogether.

Selected quench specimens were examined with both an optical microscope and a scanning electron microscope (SEM). Under a backlit optical microscope aluminum appears opaque and oxide is translucent. SEM x-ray analysis was also performed on selected samples. The analysis indicated the presence of aluminum on the portion of the particles that had been identified as aluminum. Also, oxygen was detected on the portion identified as oxide, allowing the identification of which part of the sample was aluminum and which was oxide. SEM micrographs were taken and compared with the results of the optical microscope investigation, with the SEM x-ray analysis, and with the corresponding emission trace. The results of these comparisons were used in the determination of particle burn times as discussed in the following paragraphs.

Methodology

Quenched Particle Morphology as a Function of Time

In this study, simultaneous emission traces were obtained for single, 70-μm, spherical, aluminum particles quenched at various stages of combustion in a shielded H_2/O_2 flame. Emission traces for several quenched specimens are shown in Fig. 5. The corresponding micrographs are shown in Figs. 6–9.

Figure 6 shows a 70-μm aluminum particle quenched approximately 1.5 ms following ignition. Although the particle was significantly distorted upon impact, some useful information can still be derived. Oxide smoke surrounding the particle indicates that the combustion process was well developed.

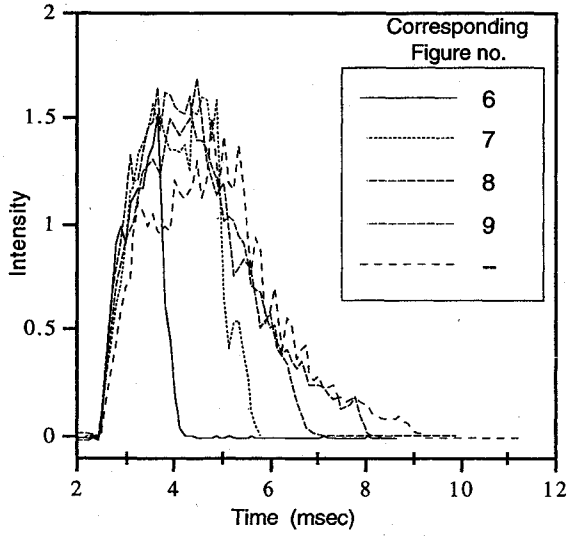

Fig. 5 Emission traces of several 70-μm aluminum particles quenched on glass slides.

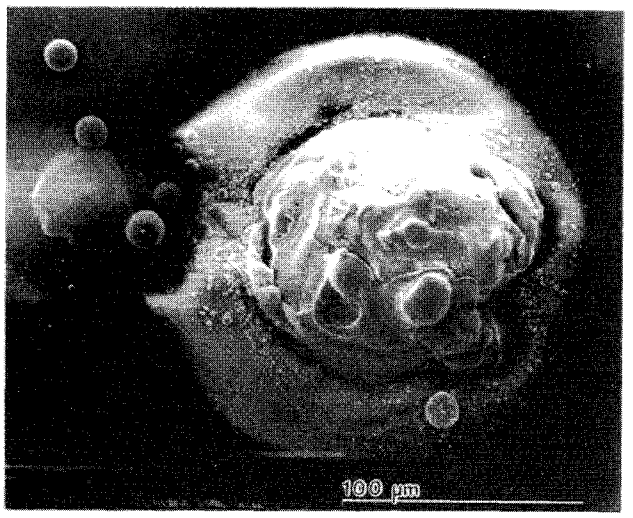

Fig. 6 SEM micrograph of a 70-μm aluminum particle quenched approximately 1.5 ms after ignition.

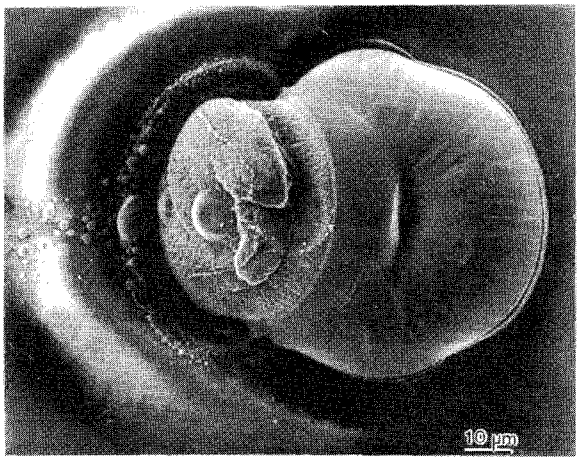

a)

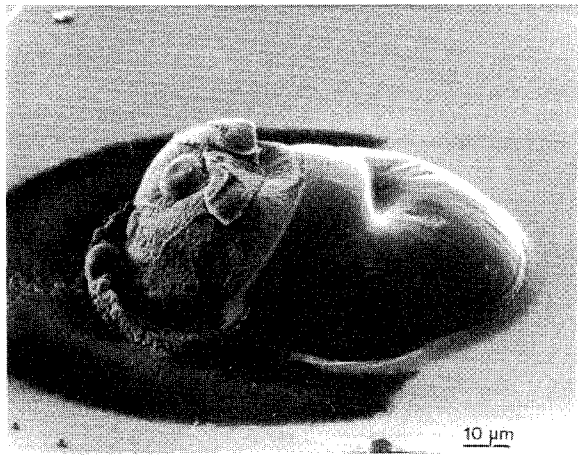

b)

Fig. 7 a) SEM micrograph of a 70-μm aluminum particle quenched 2.5–3 ms after ignition and b) SEM micrograph showing side view of particle in a).

The large mass appeared to consist mainly of what was molten aluminum, confirming that the particle was still in the early stages of combustion. No large oxide formations are obvious, although it is possible that such structures may have been distorted beyond recognition upon impact or perhaps buried beneath the mass of aluminum. Some porosity was also evident.

The particle in Fig. 7a was quenched ~2.5 to 3 ms after combustion. The same particle is shown viewed from an angle

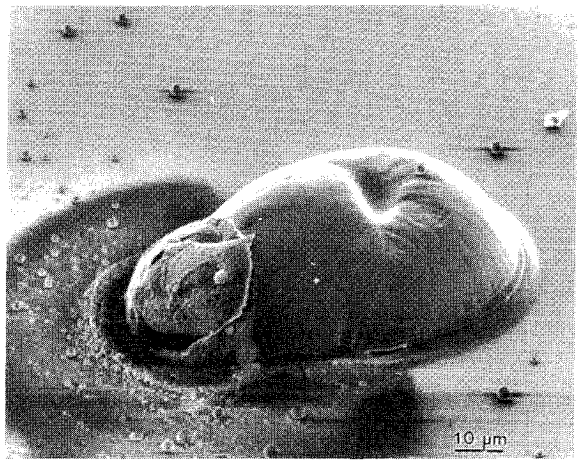

Fig. 8 SEM micrograph of a 70-μm aluminum particle quenched 4–4.5 ms after ignition.

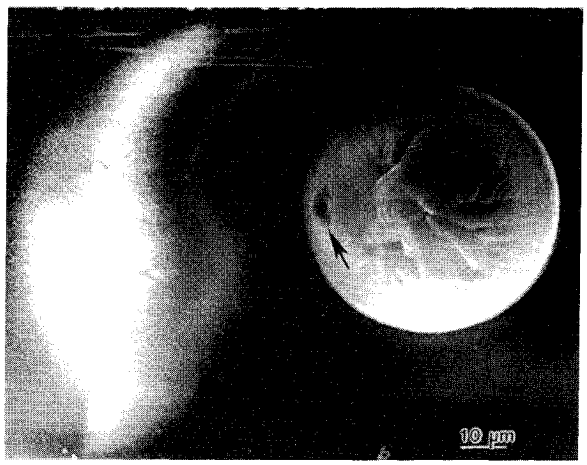

Fig. 9 SEM micrograph of a 70-μm aluminum particle quenched approximately 5.5 ms after ignition.

in Fig. 7b. The two micrographs give an idea of the distortion incurred upon impact. The dark region surrounding the left end of the particle in Fig. 7b is because of a beam specimen interaction that occurred upon tilting of the specimen. The particle morphology appears dramatically different than that shown in Fig. 6. Two distinct types of surface structure are evident upon inspection of the particle. The rougher-textured portion of the particle was identified as aluminum. The smoother portion was identified as aluminum oxide. There is good evidence to support these conclusions. First, oxide smoke particles, indicative of combustion, surround the portion of the particle identified as aluminum. The diameter of the circular smoke pattern is two to three times the diameter of the aluminum mass. This compares well to many experimental flame diameter observations (e.g., Refs. 3, 20, 23, and 24), as well as modeling calculations (e.g., Refs. 1 and 25). Second, when viewed under a light microscope, the aluminum portion appeared opaque, while the oxide appeared translucent. Third, the specimen was very similar in appearance to other quench specimens identified by x-ray analysis earlier in the study. Lastly, the conclusions are supported by similar observations of other researchers (e.g., Refs. 6, 16, and 26).

The distorted appearance of the oxide lobe indicates that it was probably somewhat soft and molten upon impact. Rough estimations indicate the remaining mass of aluminum would form a 25- to 35-μm sphere, assuming that it is solid. The appearance of other micrographs suggests the possibility of voids.

Figure 8 shows a specimen quenched after 4–4.5 ms of combustion. The overall structure appears similar to that of the preceding specimen. There has been an obvious decrease in the size of the aluminum portion of the particle, as would be expected. The aluminum appears to contain voids that may indicate that the amount of aluminum remaining is less than would be indicated by the size of the aluminum portion. If this were true, the amount of surface area exposed would be greater for a given amount of aluminum mass, increasing the rate of aluminum consumption. The possibility of voids makes it difficult if not impossible to visually estimate the amount of aluminum remaining.

The specimen in Fig. 9 burned approximately 5.5 ms before being quenched. The particle apparently consists mostly of oxide. The entire particle was translucent except for the small spot, indicated on the side of the particle, which was opaque. The presence of oxide smoke in the vicinity of the spot would indicate the possibility that it is aluminum. Although it is possible that some aluminum may be concealed beneath the oxide sphere, it appears that for practical considerations virtually all of the aluminum has been consumed.

Impact appears to have occurred ~6 to 7 ms after ignition for the final particle examined. When viewed under a light microscope, the entire particle appeared translucent. There was no visible sign of aluminum present on the particle itself. Neither was there any surrounding oxide smoke around the particle. Thus, it is concluded that combustion was complete by 7 ms.

Postcombustion Emission

Visual evidence indicates that combustion ceased as a result of aluminum depletion rather than quenching. But, the emission trace indicates the cessation of emission at the time of impact. This introduces the possibility of postcombustion emission from the hot oxide sphere. The deformation of the oxide sphere upon impact suggests that it was somewhat soft and molten at the time. It seems reasonable to assume that the highly emissive oxide sphere could be a source of significant emission at such high temperatures. Other observations made during this study support the possibility of postcombustion emission from oxide spheres. For instance, burning particles streaks often appeared yellow or orange in color near the end of combustion in contrast to the brilliant white emission observed during the majority of the process. If postcombustion emission does occur, it could be a cause of error in the determination of particle burn time, since in general, particle burn time measurements by previous investigators have been based upon either photographic or electronic detection of particle emission. These methods cannot distinguish between emission emitted by particle flame and emission from the hot oxide unless spectroscopic methods are employed.

Porous Oxide Products

Other samples collected in this study from H_2/O_2 flames have shown these residual oxide spheres to be hollow, spherical, and nearly the same size in diameter as the original aluminum particle from where they came. Several researchers have reported nearly identical findings from experiments conducted at atmospheric pressure (e.g., Refs. 5–10, 24, and 26). These hollow oxide spheres have been reported to form mainly when particle combustion occurs in environments with significant amounts of H_2 or H_2O.[23]

Researchers have also reported the formation of hollow spheres at elevated pressures. Belyeav[13] has collected hollow transparent spheres comparable in size with the starting aluminum along with fine particles less than 1 μm in diameter during propellant bomb experiments, and has published photographic evidence of these spheres with his findings. Hartman[14] reported the collection of finely divided oxide and large porous aluminum oxide particles with diameters larger than those of the initial particles from a high-pressure propellant

bomb. A micrograph of a hollow alumina sphere collected from aluminized propellant at 1000 psi has been published by Davis.[7] Hollow oxide spheres have been collected during this study from aluminum burned in an H_2/O_2 flame at 75 psi. According to Pokhil,[23] a certain part of the condensate remaining from the combustion of solid propellants is made up of hollow spheres that are virtually the same size as those obtained during burning of aluminum particles in gas burners. He also emphasized that in some cases these hollow spheres comprise a relatively small percentage of the condensate. All of this raises an interesting question. Do these hollow oxide spheres exist in rocket motors? Aluminum particle combustion products collected from rocket plumes and rotating quench bombs have shown the oxide products to be bimodal in size, consisting of small smoke particles (<2 μm) and larger oxide particles (2–100 μm), which are solid and spherical in shape.[15,21,22] Many particle damping calculations have been made, assuming the latter to be true. If hollow oxide spheres do exist in rocket motor conditions, the effect on particle damping calculations would be very significant.

Determination of Burn Time

The determination of particle burn time can be quite subjective in nature. It was found that results can differ greatly depending upon the method of analysis. The time of ignition is easily determined. The sudden increase in luminosity occurs in a fraction of a millisecond followed by a continued increase for up to a millisecond. The difficulty in measuring particle burn times lies primarily in the determination of particle burnout. It would be desirable to measure the instantaneous particle diameter and the instantaneous burn rate rather than just an overall burn time. Wilson and Williams[3] did this several years ago. However, they found that within the resolution of their photographic approach, it was virtually impossible to resolve an instantaneous burn rate. They also concluded that the rate was essentially constant. If the rate is constant, then the overall burn time approach is reasonable.

Several particle traces are shown in Fig. 10 along with a time-averaged trace. As can be seen, it is not clear where burnout occurs because of the asymptotic nature of the curve. Since the asymptotic tail makes up a significant portion of the total emission time, inclusion of the tail in burn time measurements can have a significant influence on the burn time. However, the energy release associated with the tail portion of the curve is not as significant. The determination of burn time can be complicated further by the possibility of postcombustion emission from residual oxide spheres. Previous investigators have not addressed this problem in their definitions of burn time. Either they chose to ignore the problem or were ignorant of it. To approach the problem as objectively as possible, it was decided to compare three evaluation methods to determine burn times.

Constant Intensity Cutoff Method

When determining the burn time of an aluminum particle, it is intuitive to associate the length of combustion with the length of detectable particle emission. As has been shown, this is complicated by the asymptotic nature of the emission signal. The majority of burn time data reported by other investigators has been obtained by photographic methods. In these experiments, investigators measured and compared particle burn times using film of a common sensitivity level. An analysis method similar in concept was used in this experiment. The use of a PMT allows a quantitative comparison of relative intensities between particle traces. Photographic methods do not allow a quantitative comparison.

In the first method of analysis, all particles, regardless of size or experimental conditions, were compared by measuring the time necessary to reach a common level of intensity. Because it was impossible to determine an exact intensity corresponding to particle burnout, a range of cutoff intensity was

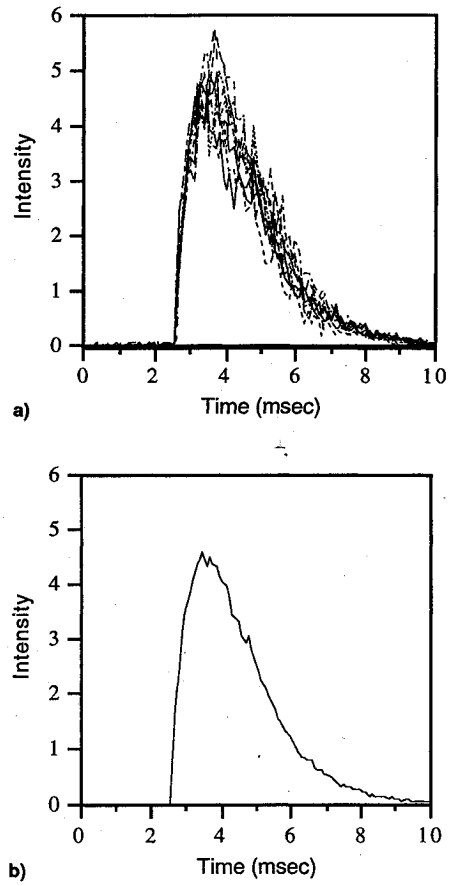

Fig. 10 a) Several 70-μm particle traces and b) time average of the traces.

determined. The burn time was defined as the amount of time for particle emission to decay to the specified range of intensity after ignition. Based on the results of the quench study, the upper cutoff limit was fixed when the amount of remaining aluminum became insignificant, from an energy release standpoint. The lower cutoff limit was set when the level of emission was considered insignificant.

Percent Peak Height Method

In recent work by Roberts et al.,[17] a shock wave was used to ignite 5000- to 10,000- (20-μm) aluminum particles at once. The burning particles produced an emission signal that was somewhat Gaussian in shape. In his experiment, particle burn times were related to a percentage of the peak intensity level. Roberts et al.[17] arbitrarily defined the burn time as the time after ignition for the signal to decay to 50% of the peak height without any justification. This is typical of previous approaches.

The concept of relating the burn time to a specified percentage of the peak intensity was applied in this study. Burn times were defined as the time necessary for the particle emission to decay to a specified percentage of its peak intensity. Data gathered from quenched particles was again used as a guide in determining a range of cutoff percentages.

Percent Total Area Method

The rate of energy release of solid propellants is of great importance. The third possibility for determination of burn times, therefore, was based upon monitoring the time release of energy during particle combustion. If it is assumed that the height of the curve (the relative intensity) is proportional to the rate of energy release occurring at the wavelengths of interest, then the area under the curve is proportional to the total energy release at those wavelengths. Burn time was then de-

fined as the time required to reach a given percentage of the total area under the curve. Burn times were evaluated at times corresponding to 95, 99, and 99.5% of the total area under the curve.

Discussion of Results

Effect of Diameter on Burn Time

Single spherical aluminum particles 40, 50, 60, 70, and 80 μm in diameter were burned in steam to determine the effect of diameter on burn time. For each datum point the emission traces of 10 particles were time averaged (Fig. 11). Burn time measurements showed good repeatability. For a sample of 10 particles, the standard deviation in burn time was typically 4–7% of the sample average. Burn time determination showed significant dependence on the particular method of analysis used.

Burn time measurements showed significant dependence on the method of analysis used. The results obtained from the constant cutoff method are shown in Fig. 12. The error bars represent the range of burn times possible from the specified relative intensity cutoff range. The upper intensity cutoff limit (given in units corresponding to Fig. 11) was set at approximately 0.3. The lower cutoff limit was set at approximately 0.05. Fitting the results obtained from the constant cutoff method to a second-order curve shows reasonable agreement with the D^2 law (Fig. 12). The error bars represent the range of burn times possible from the specified cutoff intensity range. It appears that the data trend might not pass through the origin if extrapolated to smaller diameters. The burn times for smaller particles appear long.

The results of the percent height and the percent area methods with their corresponding error bars were also examined and studied. The data are compared in Fig. 13. Both the percent height and percent area methods gave unusually long burn times for small particle sizes.

It was evident that, near the end of combustion, a significant amount of the emission time is associated with a relatively small amount of energy release. To illustrate this point, increasing the burn time cutoff point from 95 to 99% of the total area resulted in a 25% increase in measured burn time for a 70-μm particle. This could be significant for cases where the rate of energy release is of importance.

From Fig. 13 it is apparent that all three analysis methods show a clear deviation from a d^n burn rate law, particularly for small particles. This appears to be related to the unusually long apparent burn times obtained for smaller diameter particles. A careful review of the experiment was therefore conducted in an effort to identify the cause of the anomaly. The most probable cause of these results is discussed in the following text.

It was noticed that larger particles traveled a significant distance beyond the region of the ignition flame before combustion was complete, while smaller particles, having much shorter burn times, burned completely within the ignition flame region before being carried beyond the flame by postcombustion gases. It was postulated that for smaller particles, hot residual oxide spheres produced during combustion may emit significant levels of radiation following combustion until cooled in the outer regions of the ignition flame. The lengthy measured burn times were felt to be the result of postcombustion emission from residual oxide spheres.

To test the hypothesis, aluminum oxide particles, approximately the size of aluminum particles used in the experiment, were fed into the ignition flame. PMT measurements verified that oxide particles heated by the ignition flame are capable of producing significant, detectable levels of emission. This would indicate that a higher cutoff level would be justified.

All three analysis methods produced reasonable results for larger particles. The percent area method resulted in shorter burn times than the other two methods. This is the result of

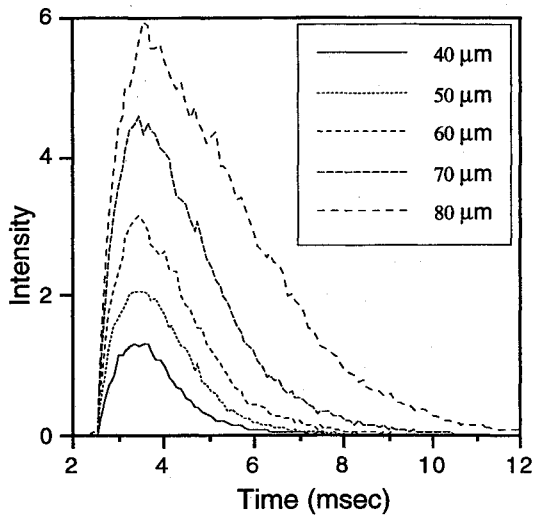

Fig. 11 Time averages of various particle diameters burned in steam.

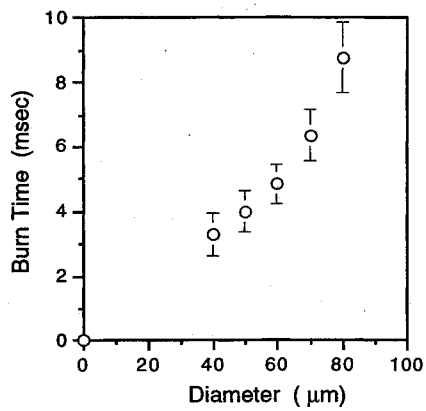

Fig. 12 Measured burn times using the constant intensity cutoff method.

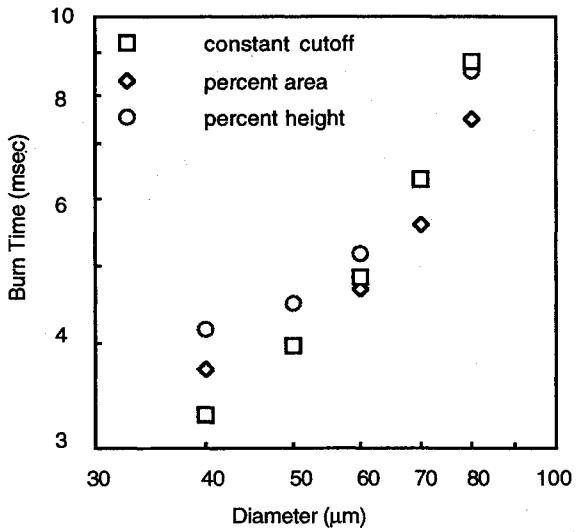

Fig. 13 Comparison of burn times determined from three data analysis methods.

the cutoff limits selected. The cutoff limits for the constant cutoff and percent height methods were determined by monitoring the mass consumption rate (via particle quench experiments). A sufficiently high cutoff limit must be selected to avoid possible confusion with postcombustion emission of the residual oxide particle. For the percent area method, the cutoff limits were defined in terms of percent total energy release.

A decision as to which method is best would depend on the application of the data. The results of the constant cutoff and percent height methods would be more suited to applications in which complete particle combustion was of importance. The percent area method might be more appropriate where the rate of total energy release is important.

Effect of Oxidizer on Burn Time

The primary oxidizers available for aluminum combustion in a rocket motor are H_2O and CO_2 (not O_2 that has been used in many previous investigations). To determine the effect of these oxidizers, single, spherical, aluminum particles (70 μm), were ignited and burned in a shielded $H_2/CO/O_2$ flame. By varying input ratios of $H_2/CO/O_2$, the oxidizer mole fraction of CO_2 in the flame combustion products was varied from 0.0 to 0.18, as shown in Table 1. Fifteen particles were burned at each condition and time averaged (Fig. 14). According to the constant cutoff intensity method, an increase in the mole fraction of CO_2 from 0.0 to 0.18 (with X_{H_2O} decreasing slightly and X_{O_2} increasing slightly) resulted in an increase of approximately 35% in burn time.

Pokhil et al.[23] have proposed a simple empirical burn law that allows for the effect of varying oxidizer concentration present during combustion[23]:

$$t_r = k(d^{1.5}/a_k^{0.9})$$

t_r is the reaction time, d is the diameter, and a_k is the sum of the mole fraction of the oxidizers including O_2, H_2O, and CO_2. This correlation implies that all oxidizers have similar effects on burn rate. However, others[18] have suggested that weighting all oxidizers equally is incorrect and propose that experimental evidence contradicts such practice. The negative effect of CO_2 addition on burn rate found in this study (Fig. 14) would support the latter view.

Brooks[1] proposed that a more appropriate correlation would be

$$t_b = A\left(d^2 \Big/ \sum c_i x_i\right)$$

where A is a constant determined from model calculations (based on ambient temperature and pressure), and c_i and x_i are the constants and mole fractions for the individual oxidizing species, respectively. The following values of c_i were suggested for conditions similar to those found in a typical burner experiment: species = H_2O, CO_2, and O_2; and for constant c_i = 0.533, 0.135, and 1.000.

According to calculations using the Brooks model,[1] increasing the mole fraction of CO_2 in a mixture of steam and CO_2 from 0.0 to ~0.18, corresponding to the data reported here, would result in a 20% increase in burn time in general agreement with the experimental data. Brooks' model also suggests that burn rate is nearly inversely proportional to the CO_2 concentration. This is also in agreement with the trends observed in this study.

Comparison to Other Experimental Data

The data collected in this work are shown plotted with data collected at atmospheric pressure by other researchers[3,4,7,8,10,12] in Fig. 15. Some burn times measured by other investigators in high oxygen concentrations were actually times to fragmentation. Those data were not included in this comparison. It can be seen that there is a great variation in burn times reported for a given diameter. This data scatter is because of variations in methods, test conditions (e.g., O_2 concentrations and am-

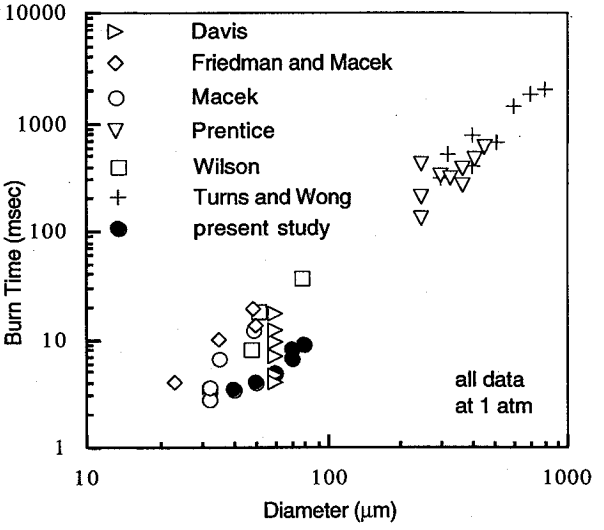

Fig. 15 Aluminum particle burn times reported by various experimenters.

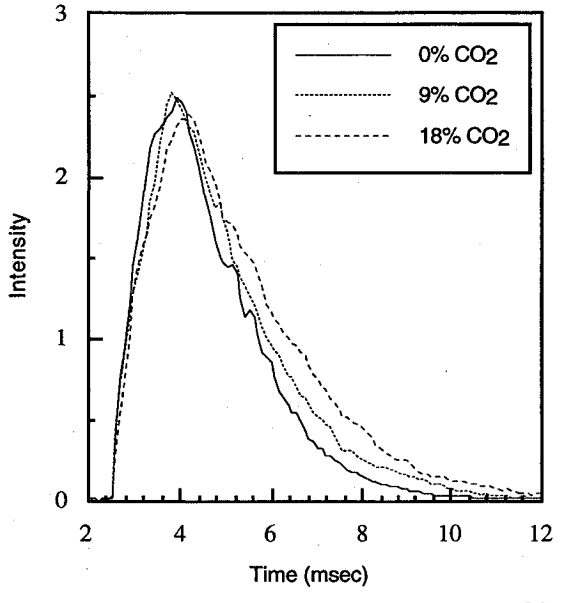

Fig. 14 Time-averaged traces of 70-μm particles burned in various CO_2/H_2O mixtures.

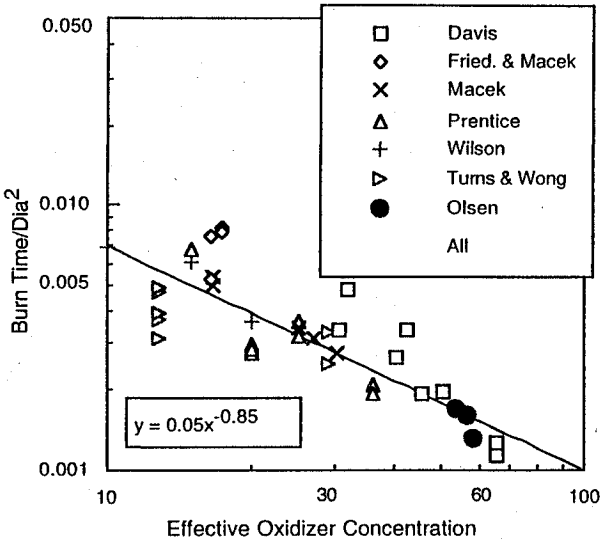

Fig. 16 Data from Fig. 15 replotted in terms of effective oxidizer concentration showing a power law fit.

bient temperatures), data reduction methods, and the use of relatively wide aluminum size distributions.

Using the c_i coefficients determined by the Brooks model,[1] and the descriptions of individual experimental conditions, CO_2 and H_2O, concentrations for each of the sets of data from Fig. 15 were converted to effective oxygen concentrations. The effective oxygen concentration was defined to be $c_{eff} \equiv \Sigma\, c_i x_i$. The data were then replotted in terms of burn time divided by the particle diameter squared vs the effective oxygen concentration in Fig. 16.

There is clearly a relationship between the burn times reported for a given diameter and the effective oxygen concentration. Increasing effective oxidizer results in a reduced burn time, which tends to explain what appears to be some of the data scatter seen in Fig. 15. The data correlate inversely with a exponent of 0.85 on the effective oxidizer concentration. It is also interesting to note that the very short burn times that were determined in this study correlate better with the other data, once the oxidizer concentration is accounted for. However, there is still significant data scatter because of the variations in methods, ambient temperatures, data reduction methods, and wide aluminum size distributions.

Summary and Conclusions

Although much work has been done in the field of aluminum particle combustion and much information has been gained, it is often difficult to compare the data of different investigators. The inherent difficulty involved in making such measurements, the various experimental techniques used, and the wide variety of conditions present during experiments have produced much scatter in the data.

In this study single aluminum particles (40–80 μm) were burned in H_2O/CO_2 mixtures, simulating a solid propellant environment. Particle emission during combustion was recorded using a PMT. In addition, single particles, quenched during combustion, were compared with simultaneous emission measurements. Quenched specimens were studied using a SEM. The combined results were used in determining particle burn times. A burn rate exponent of ~2 was calculated from the data.

Study of quenched particles revealed the formation of large hollow aluminum oxide spheres nearly the size of the original aluminum particle. These spheres have been reported by other investigators at both atmospheric and high-pressure conditions. Though not confirmed, the possibility of the existence of hollow or porous oxide spheres in rocket motors would have a significant impact on particle damping calculations. The possibility of postcombustion emission from residual oxide spheres was also apparent.

Burn time measurements depended greatly on the method of analysis used. Use of a constant intensity cutoff method gave the most reasonable results. It was also evident from this study that near the end of combustion, a significant amount of the total emission time is associated with a relatively small amount of energy release. It was found as well that increasing the mole fraction of CO_2 in flame products of CO_2/H_2O resulted in increased particle burn times. H_2O was therefore determined to be the stronger oxidizer.

Using the results of Brooks' aluminum combustion model[1] and descriptions of experimental conditions, CO_2 and H_2O concentrations were converted to effective oxygen concentrations for this work and other data. A relationship does exist between the effective oxygen concentration and burn times reported for a given diameter. The particle burn times measured in this work compare well with other data when the effective oxygen concentration is used as a basis of comparison. The short burn times measured in this study appear to be consistent because of the high effective oxygen concentrations used in this experiment.

The broad particle size distributions used in many studies are very likely a major cause of discrepancy when comparing data of various investigators. Also, the prospect of postcombustion emission from residual oxide spheres suggests a possible source of error for data in which these effects were not considered.

Acknowledgments

This research was funded by both Brigham Young University and the U.S. Air Force Office of Scientific Research Contract AFOSR-91-0152. We wish to express our sincere appreciation to Tim Parr of the U.S. Naval Air Warfare Center, China Lake for his many useful suggestions and for providing some of the equipment used in this study.

References

[1]Brooks, K. P., and Beckstead, M. W., "Dynamics of Aluminum Combustion," *Journal of Propulsion and Power*, Vol. 11, No. 4, pp. 769,770.

[2]Beckstead, M. W., and Brooks K. P., "A Model for Distributed Combustion in Solid Propellants," *27th JANNAF Combustion Meeting*, Vol. II, Johns Hopkins Univ., Columbia, MD, 1990, pp. 237–258.

[3]Wilson, R. P., Jr., and Williams, F. A., "Experimental Study of the Combustion of Single Aluminum Particles in O_2/Ar," *13th Symposium (International) on Combustion*, The Combustion Inst., Pittsburgh, PA, 1971, pp. 833–845.

[4]Prentice, J. L., "Aluminum Droplet Combustion: Rates and Mechanisms in Wet and Dry Oxidizers," Naval Weapons Center, NWC TP 5569, China Lake, CA, April 1974.

[5]Drew, C. M., Gordon, A. S., and Knipe, R. H., "Study of Quenched Aluminum Particle Combustion," *Heterogeneous Combustion*, Vol. 15, Progress in Astronautics and Aeronautics, AIAA, New York, 1964, pp. 17–39.

[6]Bartlet, R. W., Ong, J. N., Jr., Fassell, W. M., Jr., and Papp, C. A., "Estimating Aluminum Particle Kinetics," *Combustion and Flame*, Vol. 7, Sept. 1963, pp. 227–234.

[7]Davis, A., "Solid Propellants: The Combustion of Particles of Metal Ingredients," *Combustion and Flame*, Vol. 7, Dec. 1963, pp. 359–367.

[8]Friedman, R., and Macek, A., "Combustion Studies of Single Aluminum Particles," *9th Symposium (International) on Combustion*, Academic, New York, 1963, pp. 703–712.

[9]Friedman, R., and Macek, A., "Ignition and Combustion of Aluminum Particles in Hot Ambient Gases," *Combustion and Flame*, Vol. 6, March 1962, pp. 9–19.

[10]Macek, A., "Fundamentals of Combustion of Single Aluminum and Beryllium Particles," *11th Symposium (International) on Combustion*, The Combustion Inst., Pittsburgh, PA, 1967, pp. 203–213.

[11]Wong, S. C., and Turns, S. R., "Ignition of Aluminum Slurry Droplets," *Combustion Science and Technology*, Vol. 52, 1987, pp. 221–242.

[12]Turns, S. R., and Wong, S. C., "Combustion of Aluminum-Based Slurry Agglomerates," *Combustion Science and Technology*, Vol. 54, 1987, pp. 299–318.

[13]Belyaev, A. F., Frolov, Y. V., and Korotkov, A. I., "Combustion and Ignition of Particles of Finely Dispersed Aluminum," *Combustion Explosion and Shock Waves*, Vol. 4, No. 3, 1968, pp. 182–185.

[14]Hartman, K. O., "Ignition and Combustion of Aluminum Particles in Propellant Flame Gases," *8th JANNAF Combustion Meeting*, Vol. 1, Chemical Propulsion Information Agency 220, Johns Hopkins Univ., Columbia, MD, Nov. 1971, pp. 1–24.

[15]Price, E. W., Kraeutle, K. J., Prentice, J. L., Boggs, T. L., Crump, J. E., and Zurn, C. E., "Behavior of Aluminum in Solid Propellant Combustion," Naval Weapons Center, NWC TP 6120, China Lake, CA, March 1982.

[16]Tokui, H., and Iwama, A., "X-Ray Microanalysis on the Surface and Cross-Section of Burning-Interrupted Aluminum Particle and Foil in High Pressure Atmospheres," *Propellants, Explosives, Pyrotechnics*, Vol. 14, 1989, pp. 127–132.

[17]Roberts, T. A., Burton, R. L., and Krier, H., "Ignition and Combustion of Aluminum/Magnesium Alloy Particles in O_2 at High Pressures," *Combustion and Flame*, Vol. 92, 1993, pp. 125–143.

[18]Micheli, P. L., and Schmidt, W. G., "Behavior of Aluminum in Solid Rocket Motors," Edwards AFB, AFRPL-TR-76-58, Edwards, CA, Jan. 1977.

[19]Price, E. W., Christensen, H. C., Knipe, R. H., Drew, C. M., Pren-

tice, J. L., and Gordon, A. S., "Aluminum Particle Combustion Progress Report," Naval Ordnance Test Station, NOTS TP 3916, China Lake, CA, 1965.

[20]Prentice, J. L., and Kraeutle, K. J., "Metal Particle Combustion Progress Report," Naval Weapons Center, NWC TP 4658, China Lake, CA, 1968.

[21]Braithwaite, P. C., Christensen, W. N., and Daugherty, V., "Quench Bomb Investigation of Aluminum Oxide Formation from Solid Rocket Propellants (Part I): Experimental Methodology," *25th JANNAF Combustion Meeting*, Vol. 1, Johns Hopkins Univ., Columbia, MD, 1988, pp. 175–184.

[22]Salita, M., "Quench Bomb Investigation of Aluminum Oxide Formation from Solid Rocket Propellants (Part II): Analysis of Data," *25th JANNAF Combustion Meeting*, Vol. 1, Johns Hopkins Univ., Columbia, MD, 1988, pp. 185–198.

[23]Pokhil, P. F., Belyayev, A. F., Frolov, Y. V., Logachev, V. S., and Korotkov, A. I., "Combustion of Powdered Metals in Active Media," Foreign Technology Div., FTD-MT-24-551-73, Wright–Patterson AFB, OH, Oct. 1973.

[24]Arkhipov, V. A., Ermakov, V. A., and Razdobreev, A. A., "Dispersity of Condensed Products of Combustion of an Aluminum Drop," *Combustion, Explosions and Shock Waves*, Vol. 18, No. 2, 1982, pp. 16–19.

[25]Law, C. K., "A Simplified Theoretical Model for the Vapor-Phase Combustion of Metal Particles," *Combustion Science and Technology*, Vol. 7, 1973, pp. 197–212.

[26]Drew, C. M., Gordon, A. S., Knipe, R. H., Kraeutle, K. J., Prentice, J. L., and Price, E. W., "Metal Particle Combustion Progress Report," Naval Weapons Center, NWC TP 4435, China Lake, CA, 1967.